UNIVERSITY OF BIRMINGHAM

Monte Carlo Simulations of an F_0F_1 ATP Synthase Model: A Study of coupled Molecular Motors

Nils Gustafsson - 1066960

Issue: 1
Date: January 14, 2013

School of Physics and Astronomy
University of Birmingham
Birmingham, B15 2TT
E-Mail: nsg960@bham.ac.uk

Abstract

A model for F_0F_1ATP Synthase as two chemically driven ratchets with constant forward rates in opposing directions coupled by an elastic axle in a 'tug of war' is proposed. A Monte-Carlo method is used to simulate the operation of this model to study the rate dependence on the free energy available to the F_0 motor and the torsional rigidity of the axle. The rate of synthesis is found to agree quantitatively in the thermodynamic limit and in the maximum rate to experimental data. Good qualitative agreement is found away from these limits. Three Phases of operation are observed, a forward synthesis phase, a backward proton pumping phase and a locked phase. A mean field theory for the model is discussed and provides a basis for the onset of these phase transitions. A possible model for a rate limiting process with an analytical solution is proposed although not rigorously formulated. Auto-correlation and frequency analysis of the transition sequence identifies two operating regimes between which the model transitions smoothly at the phase transition. These are, a highly correlated regime characterized by alternate stepping and a single frequency peak in a low background of white noise, and an uncorrelated regime characterised by transition fluctuations which obey Brownian statistics. Word Count ∼7000

Keywords: F_0F_1 ATP Synthase; Biological Nano-motors; Thermodynamics; Random Walk; Monte-Carlo Simulation; Torsional Rigidity; Synthesis Rate; Correlation

---

I would like to acknowledge the contribution of Dr N. Thomas whose proposal of the project and guidance have made this work possible. I would also like to acknowledge Dr W. Theis for his supervision of the project and the seminars and Dr C Mayhew and the University of Birmingham for the running of the 4th Year Projects.

Contents

List of Figures

1 Introduction

Adenosine triphosphate (ATP) is often quoted as being the energy currency of life [Walker, 1997]. The hydrolysis of ATP into adenosine diphosphate (ADP) and an inorganic phosphate,

$$ATP \rightarrow ADP + P_i, \tag{1}$$

liberates free energy [Lipmann, 1941]. The free energy from this reaction is used in muscle, brain, nerve, kidney, liver and other tissues for a multitude of tasks including molecular transport, force generation and bio-synthesis [Boyer, 1997b]. So much ATP is required in the human body that of the order of $2\text{x}10^{26}$ molecules or equivalently 160kg of ATP can be synthesized from ADP and P_i daily [Karp, 2008]. Boyer [1997b] estimates that, as nearly all living organisms rely on ATP hydrolysis, the net synthesis of ATP is the principal chemical reaction in the world. It is clear from this that a full understanding of the process by which ATP is synthesized is of great importance.

In this project a discussion of experimental work to date and the thermodynamics of biological nano-motors forms the basis for the proposal to model F_0F_1 ATP Synthase (ATPase), the enzyme responsible for the catalysis of the ATP synthesis reaction, as two rotary biological nano-motors coupled by an elastic axle. Monte Carlo simulations of random walk and a chemically driven ratchet inform the development of a simulation of the ATPase model proposed. A User interface for the demonstration of this simulation is included in a single application, ATPase Application, written in the multi-paradigm programming language C# developed by Microsoft and designed for the Common Language Infrastructure used by the .Net Framework [MSDN Website, 2012]. Command line driven versions of the simulation, writen in C++, were used to collect large data sets to study the rate of ATP synthesis and the correlation of the two coupled motors.

1.1 F_0F_1 ATP Synthase

F_0F_1 ATP Synthase (ATPase) is an enzyme whose main function is to synthesis ATP from ADP and P_i. Motivation for the study of ATPase however goes beyond the importance of the synthesis of ATP. It is remarkably

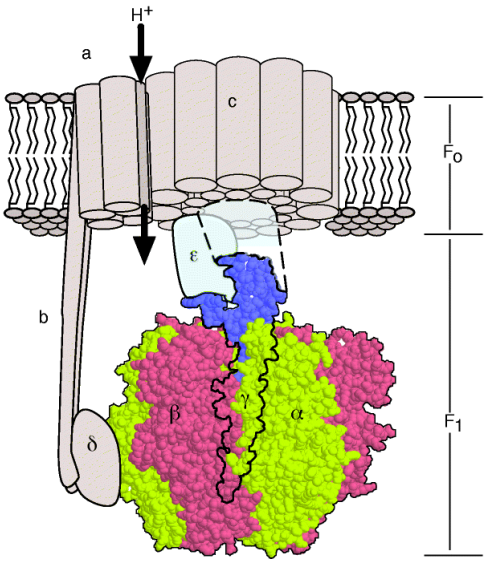

Figure 1: Protein structure of F_0F_1 ATP Synthase [Columbia University, 2011]

conserved in evolutionary terms and is ubiquitous in bacterial cell membranes, the thylakoid membranes of chloroplasts and the inner membranes of mitochondria. It is implicated in many physiological roles and is likely to be a target for both therapeutic drugs and the phagocytosis of cancerous cells by $\gamma\delta$T cells [Mookerjee-Basu et al., 2010] and the inhibition of ATPase may also be useful in preventing tissue damage during ischemia.

Boyer [1997a] gives a comprehensive proposal for the mechanism by which ATPase catalyses the synthesis of ATP and the structure (figure 1) [Walker, 1997] [Walker et al., 1999] confirms these hypotheses. In summary the ATPase consists of two distinct biological nano-motors. The membrane embedded F_0 rotary motor consists of between 9 and 15 c-subunits which are driven in a turnstile like manor [Berry, 2000] by the proton gradient across the membrane. This proton gradient is formed by the oxidation of food molecules driving the electron transport chain in mitochondria, or by photosynthesis in chloroplasts [Nicholls and Ferguson, 1992]. The rotary motion is then transfered to the γ-subunit of the F_1 which acts as an axle while the F_0 a,b-stator holds the $\sim$10nm diameter hexagonal $\alpha_3\beta_3$ protein complex in place. The rotation of the asymmetric γ-subunit causes conformational changes in $\alpha_3\beta_3$ changing the binding affinity of ATP, ADP and P_i resulting in the catalysis of ATP synthesis [Boyer, 1997a]. The coupling of these two motors is important as the F_1 motor in isolation would hydrolyse ATP as per equation 1 rotating the γ-subunit as observed by Kinosita et al. [1998a]. This is the desired effect in some bacteria which use ATPase as a proton pump to maintain inter membrane proton concentrations. For ATP synthesis however, it is only the free energy obtained from the proton gradient by the F_0 motor, transfered via the rotary motion of the axle to the F_1 motor, that allows it to work in reverse and synthesis ATP.

1.2 Biological Nano-Motors

Motion and the ability to perform mechanical work on a molecular scale in biological systems is important in almost every function of life and is performed by proteins called molecular motors or biological nano-motors. Some extensively studied examples include actomyosin, responsible for muscle contraction [Thomas and Thornhill, 1997] [Huxley, 1969] as well as myosin V [Rief et al., 2000] [Walker et al., 2000] and kinesin [Howard et al., 1989] which are molecular tethers and transporters respectively. While a macroscopic heat engine can harness free energy and produce useful work through the application of a thermodynamic cycle, a biological nano-motor can perform useful work by harnessing chemical free energy available through a biochemical cycle. The molecular scale environment however is characterised by the presence of nonzero temperature particles performing Brownian motion as per the thermal bath described by Bobylev and Cercignani [2002]. In these conditions fluctuations due to thermal noise become significant leading to the biological nano-motors exhibiting stochastic behavior and a motion which can be described by a biased random walk [Berg, 1993].

1.3 Biased Random Walk

A random walk can be demonstrated by considering a protein attached at position n, to a one dimensional track of discrete step size u_0, which steps between sites with a forward rate of k_+ and a backward rate k_- (figure 2). In a time δt the number of forward steps is given by $k_+\delta t$ and the number of backward steps is given by

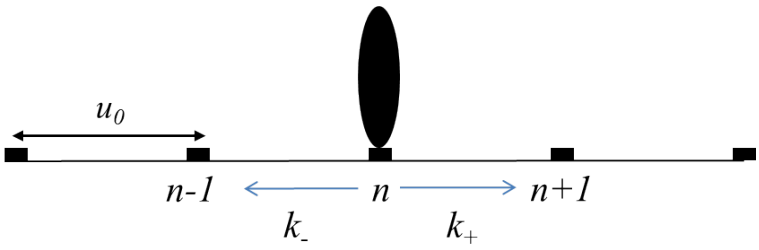

Figure 2: Protein on a one dimensional track

$k_-\delta t$ which are also the probabilities δp_+ and δp_- of a forward or backward step respectively in the time δt. It follows that the average stepping velocity is given by

$$v = \frac{\delta x}{\delta t} = u_0(k_+ - k_-), \tag{2}$$

and the diffusion constant D can be calculated from

$$\langle \delta x^2 \rangle = u_0^2 k_+ \delta t + u_0^2 k_- \delta t \tag{3}$$

$$= u_0^2(k_+ - k_-)\delta t, \tag{4}$$

and the diffusion equation

$$\langle \delta x^2 \rangle = 2D\delta t \tag{5}$$

$$\Rightarrow D = u_0^2(k_+ - k_-)/2 \tag{6}$$

[Thomas, 2011b].

1.4 Chemically Driven Ratchet

If the protein considered in Section 1.3 is subject to a load f, linked to a chemical reaction $A + B \leftrightarrow C + D$ per step and constrained to never leave the track, we say it is a tightly coupled, processive molecular motor (figure 3). In this case the forward rate k_+ and the backward rate k_- may be dependent on any number of factors

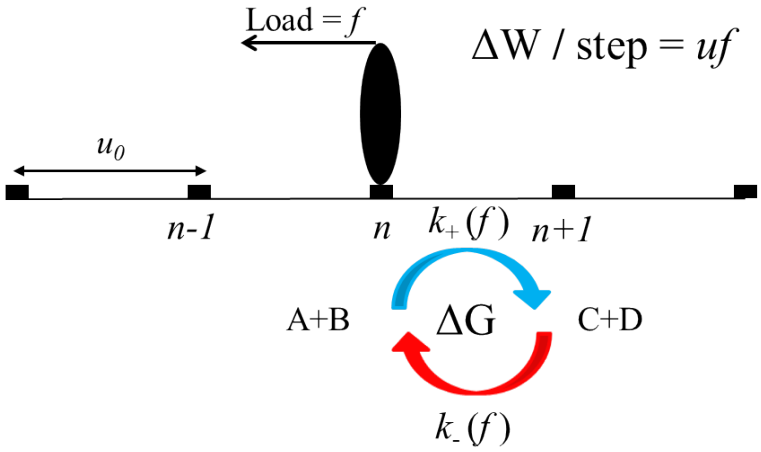

Figure 3: One dimensional chemical ratchet

intrinsic to the inner workings of the motor, for example the load dependences of binding or reaction rates, but thermodynamics imposes a strict constraint on the ratio k_+/k_-. Consider the law of mass action applied to the reaction in figure 3

$$k_+/k_- \propto [A][B]/[C][D], \tag{7}$$

where [A] denotes a concentration of reactant A.

Taking the change in the Gibbs free energy for the reaction to be

$$\Delta G = \Delta G' + k_B T ln\left([C][D]/[A][B]\right), \tag{8}$$

where $\Delta G'$ is the standard free energy of the reaction, k_B is the Bolzmann constant and T is the temperature, it follows from equations 7 and 8 that

$$k_+/k_- = a \exp\left[-\Delta G/k_B T\right], \tag{9}$$

where a is a constant of proportionality. Note that if this free energy change, ΔG, is negative the reaction will proceed spontaneously [Thomas, 2011a]. Einstein's principal of detailed balance states that when the cycle is in thermodynamic equilibrium the forward and backward rates must be equal. The work done, ΔW, per forward step is $u_0 f$ (figure 3) so the motor is in thermodynamic equilibrium when this is equal to the free energy change per step, $-\Delta G$. Hence, $a = \exp -u_0 f/k_B T$ and the ratio of the rate constants must obey

$$k_+/k_- = \exp\left[-(\Delta G + \Delta W)/k_B T\right] \tag{10}$$

$$= \exp\left[-(\Delta G + u_0 f)/k_B T\right], \tag{11}$$

in order to satisfy the thermodynamics of the system.

Two of the idealised cases discussed by Thomas et al. [2001], for which the velocity dependence on load can be solved analytically, are presented here.

Case A

If the backward rate, k_-, is held constant and independent of the load, f,

$$k_+ = k_- \exp\left[-(\Delta G + u_0 f)/k_B T\right]). \tag{12}$$

and the average velocity of the motor (equation 2) is given by

$$v = u_0 k_- (\exp\left[-(\Delta G + u_0 f)/k_B T\right] - 1). \tag{13}$$

Case B

Conversely, if the forward rate, k_+, is held constant and independent of the load, f,

$$k_- = k_+ \exp\left[(\Delta G + u_0 f)/k_B T\right]). \tag{14}$$

and the average velocity of the motor is given by

$$v = u_0 k_+ (1 - \exp\left[(\Delta G + u_0 f)/k_B T\right]). \tag{15}$$

Figure 4 shows the form of these functions for the arbitrary values $\Delta G = -10$kJ M^{-1} and $u_0 = 1$ nm. The value for $k_B T = 4.28$ pN nm in biological systems is calculated using a temperature of 37^oC. Figure 4a uses a constant $k_- = 1s^{-1}$ and figure 4b uses a constant $k_+ = 1s^{-1}$. Both cases show an equilibrium value $f = -\Delta G/u_0 = 10$ pN and are driven forwards spontaneously forwards by the free energy available from the biochemical cycle, hence performing work, when $u_0 f < -\Delta G$. As such, both may be considered chemically driven ratchets but

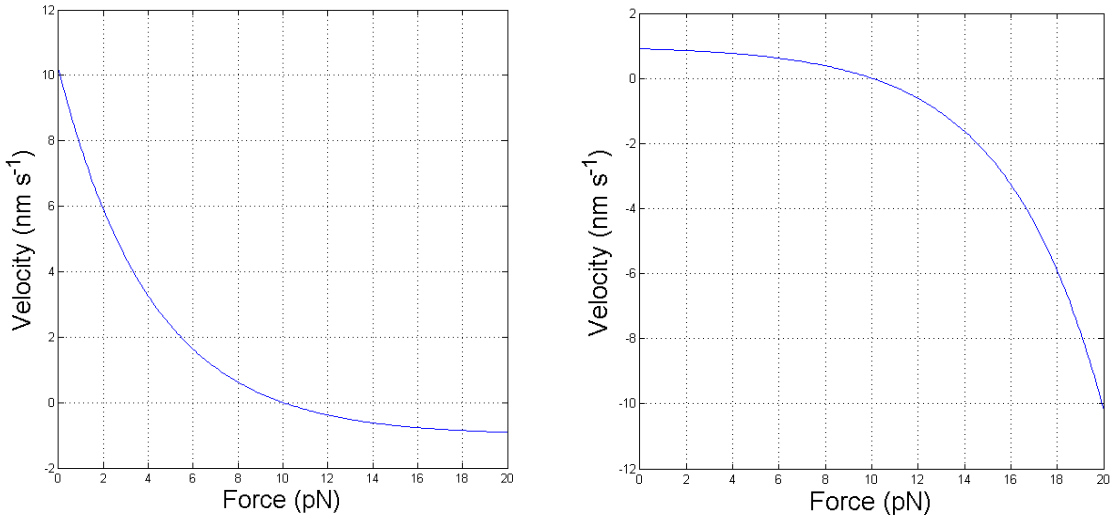

(a) A-Type Motor: constant $k_- = 1s^{-1}$ (b) B-Type Motor: constant $k_+ = 1s^{-1}$

Figure 4: Velocity against load for chemically driven ratchets

with reversed polarity.

The forward velocity of the B-type motor at $f = 0$ is given by $v = u_0 k_+(1 - \exp[\Delta G/k_B T])$ and approaches a maximum forward velocity $v = u_0 k_+$ for $-\Delta G \gg k_B T$ or $f \to -\infty$. Similarly, for the A-type motor the maximal backward velocity approaches $v = -u_0 k_-$ as $f \to +\infty$. The backward rate of the B-type motor however is theoretically unbounded under increasing load. If the F_1 were to behave as a B-type motor the backwards force provided by the rotation of F_0 would produce very fast ATP synthesis.

1.5 F_0F_1 ATP Synthase Model

Kinosita et al. [2005] and Junge et al. [2008] have shown that it is possible to perform experiments on the entire F_0F_1 ATP Synthase molecule however neither of these experiments were able to study ATPase *in vivo* or with the F_0 portion embedded in a membrane. The work by Kinosita et al. [2005] does however confirm that the [ATP] dependence and maximal hydrolysis rate of the F_1 motor, which has been extensively studied in isolation, does not change with when the F_0 motor is attached but not membrane bound. This confirms that it is not unreasonable to construct a model of ATPase by considering the properties of the F_0 and F_1 motors separately. Following which, the work by Junge et al. [2008] will inform the coupling of the two motors with data on the torsional rigidity of the γ-subunit. Furthermore the structure of both the F_0 and F_1 motors in ATPase strongly suggest a tightly coupled and processive type behavior as discussed in section 1.4 [Berry, 2000] and as such will obey the thermodynamic relation given in equation 10. This thermodynamic relation will form the theoretical basis for the ATPase model.

Kinosita et al. [1997] is the first prominent study of F_1 in isolation. The F_1 motor was isolated and the $\alpha_3\beta_3$ complex was tethered in place by His-tags. A fluorescent actin filament was attached to the γ-subunit using

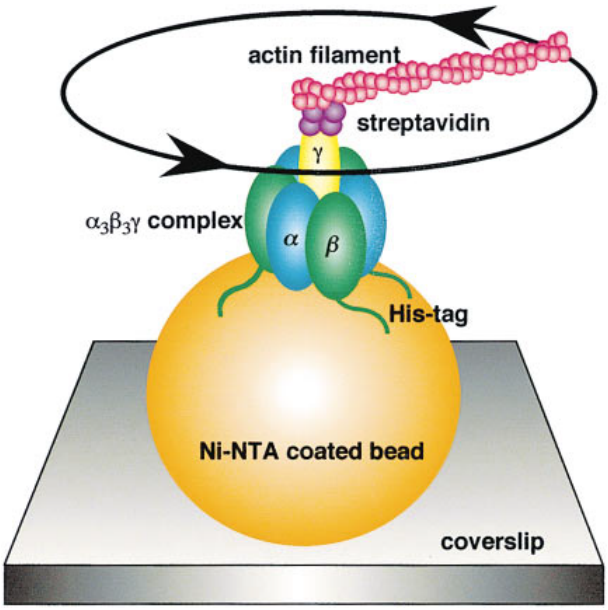

Figure 5: Immobilised F_1 showing rotation of the γ-subunit via the attachment of a florescent actin filament [Kinosita et al., 1998b]

streptavidin and its rotation was observed in the presence of ATP (figure 5). This method allows for the calculation of the force dependence of the velocity by varying the actin filament length. This work and other studies since provide data which suggests the behavior of the F_1 is remarkably like that of the B-type chemically driven ratchet (section 1.4) with a discrete step size of 120^o per ATP hydrolysis [Kinosita et al., 1998a] [Kinosita et al., 1998b] [Kinosita et al., 2000] and a maximal velocity $v_{max} \approx 352 \pm 16$ revolutions per second [Kinosita et al., 2005]. From this we determine that the rate constants for the F_1 motor will be $k_+ \approx 1050s^{-1}$ and k_- will be given by equation 14.

Very little reliable experimental evidence for the force dependence of the velocity of the membrane embedded F_0 motor is currently available. The bacterial flagellar motor however, an ion driven rotary motor responsible for bacteria motility, which is very similar in its structure and function to the F_0 motor has been studied extensively. Berry et al. [2000] has shown that the flagellar motor may have a constant k_+ and exhibit B-type behavior with $v_{max} \approx 303 \pm 35$ revolutions per second. Translating this to an F_0 motor with 10 c-subunits we estimate k_+ to be of the order of $2680 - 3380s^{-1}$ a claim supported by the rates observed by Lill et al. [1989]. The more recent study by Deckers-Hebestreit and Altendorf [1992] however suggests values of $100 - 120s^{-1}$ for k_+. It is apparent the the method used for the preparation of the F_0 motor for experiment has a large effect on its operation and as such k_+ cannot be defined at this point. We are confident however that F_0 behaves analogously to a B-type motor.

With the assumption of B-type behavior for the two individual motors in ATPase we construct a model of ATPase as a 'tug of war'. Figure 6 shows this model diagrammatically as two linear motors on separate tracks. The l_0 motor represents the F_0 portion of ATPase with forward steps of size u_0 in the direction of $n + 1$ at

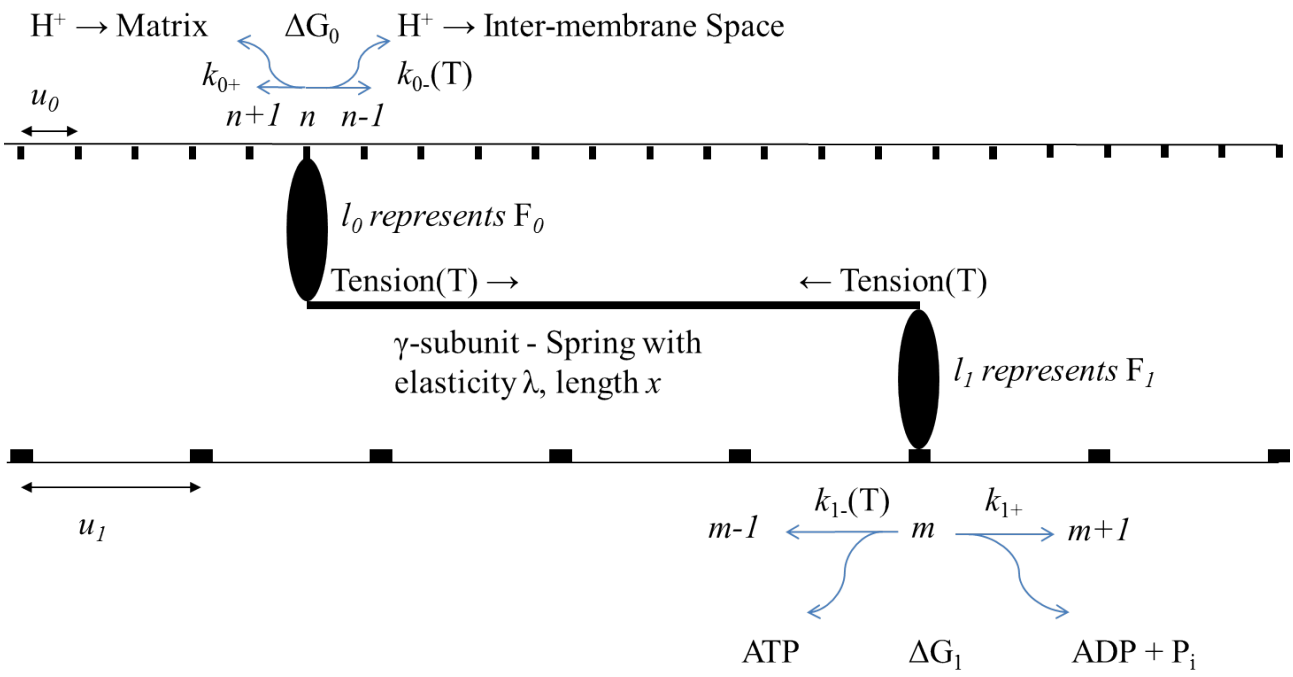

Figure 6: Linear Analogue of the ATPase

a rate k_{0+} yet to be determined. These forward steps are coupled to a single proton transport from the inter membrane space to the F_1 matrix side of the membrane with free energy change ΔG_0. The l_1 motor represents the F_1 portion of ATPase with forward steps of size u_1 in the direction of $m+1$ at a rate k_{1+} coupled to a single ATP hydrolysis reaction releasing ΔG_1. As both of these motors will be modeled by the B-type chemically driven ratchet the backward rates have the form

$$k_{i-} = k_{i+} \exp\left[(\Delta G_i + \Delta W_i)/k_B T\right], \tag{16}$$

as per equation 14. The work done per step is determined by the change in the length, x, of the spring coupling the the two motors when a backwards step is made

$$\Delta W_i = \frac{1}{2}\lambda(x^2 - (x - u_i)^2). \tag{17}$$

This implies

$$k_{i-} = K_{i+} \exp\left[\lambda u_i x/k_B T\right], \tag{18}$$

where x is the instantaneous spring length calculated from the positions of the two motors and

$$K_{i+} = \exp[(\Delta G_i - \frac{1}{2}\lambda u_0^2)/kT]. \tag{19}$$

A selection of arbitrarily chosen parameters will be used to characterise the behavior of this model but a specific set of parameters used to study the model under biological conditions will be outlined here.

The rate constants k_{0-} k_{1+} and k_{1-} will be as discussed previously while the F_0 forward rate constant, k_{0+}, will be discussed in section 1.6. The parameters chosen will reflect the fact that in a biological system ATPase is rotary in nature although in essence the model is still a linear analogue. The step size u_1 will be $2\pi/3$ rad and the step size u_0 will be $2\pi/10$ rad and $2\pi/14$ rad for human and chloroplast ATPase respectively. The free energy ΔG_1 for ATP hydrolysis is determined using equation 8 for the reaction given in equation 1. The concentrations used are those typically found in human mitochondria and give a value $\Delta G_1 \approx -48$ kJ M^{-1}. The free energy provided by the trans membrane electro chemical proton potential difference [Nicholls and Ferguson, 1992] is given by

$$\Delta G_0 = -F\Delta\psi + 2.3RT(\mathrm{pH}_p - \mathrm{pH}_N) \tag{20}$$

where F is the Faraday constant, ψ is the trans membrane potential difference and pH_p and pH_N are the pH values on the positive and negative sides of the membrane respectively. Typical values in biological systems are between -11 and -20. The final parameter to consider is the elasticity of the γ-subunit which in rotational terms is a torsional rigidity. The most reliable experimental value for the torsional rigidity found is that given by Junge et al. [2008] who, having removed the ATPase from the membrane, observed the angular fluctuations of a bead attached to the F_0 motor in the absence of a proton drive while the F_1 was at each of its 120^o sites. They cite a value of 68 pN nm rad^{-1} for the most complaint part of the axle. Other work, [Pänke and Rumberg, 1999] and [Junge et al., 1999] suggests values of 30 pN nm rad^{-1} and 60 pN nm rad^{-1} respectively.

1.6 Pseudo Mean Field Theory

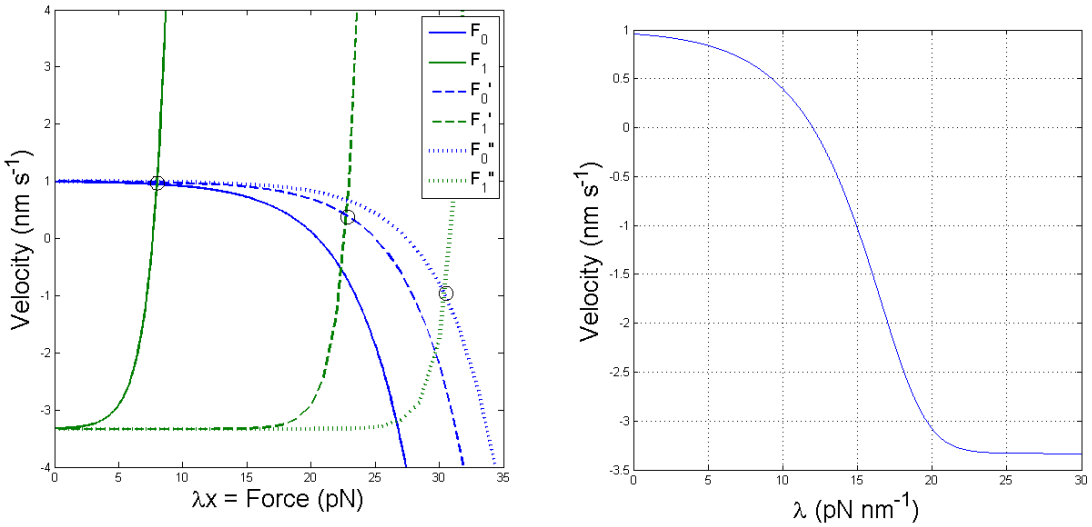

(a) F_0 and F_1 velocity against spring tension at three values of λ

(b) ATPase velocity against λ

Figure 7: Mean field Theory

The instantaneous velocities of the two motors in the positive n direction are shown in figure 7a. These were calculated for arbitrary values $\Delta G_0 = \Delta G_1 = -20$kJ M^{-1}, $u_0 = 1\ nm, u_1 = 3.333\ nm$, $k_{0+} = k_{1+} = 1\ s^{-1}$

at three values of λ, 1 pNnm^{-1}, 10 pNnm^{-1} and 15 pNnm^{-1} using equation 2 and 18. The intersections of these pairs of curves indicated by the circles in figure 7a give the 'operating points' of the ATPase at different λ, from which it is proposed the rate of ATP synthesis can be calculated. This treatment yields the velocity of the ATPase for varying λ given in figure 7b. However, when one motor makes a step the length of the spring changes creating a fluctuation in the force on the other motor. These fluctuations around the operating point along the path of the force velocity curves are approximated to an effective mean tension in this analysis. We therefore expect this model (as with other mean field theories [Lerner, 2011]) to deviate from the actual behavior of ATPase at large λ when the fluctuations will be significant. Furthermore the negative velocities seen at larger values of λ are not possible thermodynamically for the given values of the free energies and step sizes.

At small values of λ however we expect this method to be accurate. This is an important observation as at $\lambda \to 0$ the mean field theory (MFT) suggests the maximal velocity of the ATPase is limited by and equal to the maximal velocity of the F_0 motor. This allows us to determine the k_{0+} rate constant from the maximal velocity of the ATPase for which there is more comprehensive experimental data. For example, Junesch and Graber [1991] find a maximal ATP synthesis rate of $\approx 380 \pm 20$ per second equivalent to a maximum velocity of 125 revolutions per second. This gives a k_{0+} constant of approximately $1300s^{-1}$ for F_0 with 10 c-subunits or a rate of $1820s^{-1}$ for F_0 with 14 c-subunits as in ATPases found in chloroplasts.

Having determined rates for all four of the possible transitions in the model it is possible to use a Monte-Carlo method to simulate the behavior of this model.

2 Methodology

2.1 Monte Carlo Simulations

In general a Monte Carlo (MC) method is a statistical method proposed by Metropolis and Ulam [1949] for the study of differential equations and are most useful for the study of systems which are insoluable analytically. They are more commonly thought of however as a class of computational algorithms useful for stochastic simulations of systems which behave like a Markov Chain, a random process where the next state in the chain depends only on the current state. An MC simulation often follows a generalised pattern of implementation consisting of, repeated random sampling from a probability distribution over a defined domain, with a deterministic computation performed on each of the random samples, before aggregating the results.

MC Algorithms rely heavily on truly random sampling as very large numbers of samples are often required to produce reliable results. As such a high quality pseudo random number generator proposed by Matsumoto and Nishimura [1998], quoted as having a period of $2^{19937} - 1$ and equidistribution across 623 dimensions with minimal computation, was used.

For the specific case of the random walk outlined in section 1.3 the MC algorithm implemented in ATPase Application is provided in Appendix A.1 the form of which is as follows.

In time δt the probability of a forward step is given by $k_+\delta t$ while the probability of a backward step is given $k_-\delta t$. These probabilities divide the domain of a uniform probability distribution as shown in figure 8. A random number r is sampled from this uniform probability distribution in the domain [0,1]. A logic check is

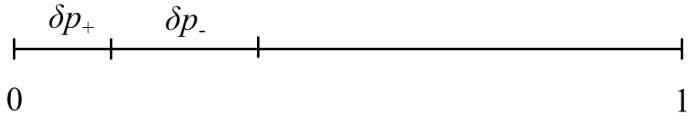

Figure 8: The domain of the probability distribution for the Monte Carlo simulation

performed on the random number to determine if it lies in the δp_+ region, the δp_- region or outside of either indicating no transition has occurred in δt. The position of the protein on the track is altered accordingly and the process repeated. The selection of the value of δt is vital to the success of this method. It must be small enough that $\delta p_+ + \delta p_- < 1$ but also it must be small enough that the probability of two steps occurring in δt is insignificant. If the probability of a single transition occurring in δt ($\delta p_+ + \delta p_-$) is 0.1 then the probability of two transitions in δt is 0.01. On average, this will lead to 1 in 10 cases where a single transition has occurred when a pair of transition should have occurred. However the significance of this effect can be reduced by reducing the probability of a single transition as the probability of a pair of transitions is proportional to the square of the probability of a single transition. For $\delta p_+ + \delta p_- = 0.001$ the probability of two transitions in δt is 10^{-6}. This still means 1 in 1000 single transitions should be double transitions but this is an acceptable reduction in the significance of the effect. A suitable time step can be calculated using

$$\delta t = 0.001 / \sum_i k_i \tag{21}$$

where $\{k_i\}$ is the set of rate constants for the possible transitions. If the rate constants change between transitions as in the case of the ATPase model this time step δt is calculated dynamically.

On average this algorithm performs 1000 random samples for every transition which is computationally heavy resulting in long run times for a representative sample of transitions. For this reason a second algorithm based on the dwell time between transitions has been developed which requires only two random number samples per transition (Appendix A.2).

To formulate this algorithm a more vigorous treatment of the transition probabilities is provided. Let us assume we know $p_n(t)$ the probability of finding the protein at site n for a specific time t. At $t' = t + \delta t$, $p_n(t+\delta t) = p_n + \Delta$ where Δ is some small correction. δt is assumed to be small again such that the probability

of two transitions in the time δt is small. So we can write

$$\begin{aligned} p_n(t+\delta t) = \text{Prob}[n(t) = n \text{ and no event has occurred}] \\ +\text{Prob}[n(t) = n\text{-}1 \text{ and a forward step has occurred}] \\ +\text{Prob}[n(t) = n{+}1 \text{ and a backward step has occurred}]. \end{aligned} \tag{22}$$

We assume a Markov Chain process which allows us to say these three probabilities are mutually exclusive, so sum to 1, are independent of n and proportional to δt. This allows us to write

$$\begin{aligned} p_n(t+\delta t) &= p_n(t)(1-(k_+ + k_-)\delta t) + p_{n-1}(t)k_+\delta t + p_{n+1}(t)k_-\delta t \\ &= p_n(t) + \delta t[k_+ p_{n-1}(t) + k_- p_{n+1}(t) - (k_+ + k_-)p_n(t)] \end{aligned} \tag{23}$$

which implies if we know $p_n(t)$ for all n at a given t we can find the probability of site occupation at any later times. Equation 23 is in fact the forward Euler method for finding the solution, numerically, to the differential equation produced by taking the limit when $\delta t \to 0$

$$\lim_{\delta t \to 0} \frac{p_n(t+\delta t) - p_n(t)}{\delta t} = \frac{dp_n(t)}{dt} = -(k_+ + k_-)p_n(t) + k_+ p_{n-1}(t) + k_- p_{n+1}(t) \tag{24}$$

Now consider at time $t = 0$ the position of the protein is known, $p_0(0) = 1$. The Dwell time at this position is assigned the random variable $\mathcal{T}$ with probability density $\mathcal{F}_\mathcal{T}(t)$ and the probability that no event occurs in time $(0, t)$ is given by $q(t)$. From equation 24 we have

$$\begin{aligned} \frac{dq(t)}{dt} &= -(k_+ + k_-)q(t) \\ \Rightarrow q(t) &= \exp\left[-(k_+ + k_-)t\right] \end{aligned} \tag{25}$$

from which the probability of at least one event in $(0, t)$, is given by $1 - q(t)$ hence we can determine $\mathcal{F}_\mathcal{T}(t)$.

$$\begin{aligned} 1 - q(t) = \text{Prob}[\text{Dwell Time } \mathcal{T} < t] &= \int_0^1 \mathcal{F}_\mathcal{T}(t')dt' \\ \Rightarrow \mathcal{F}_\mathcal{T}(t) &= (k_+ + k_-)\exp\left[-(k_+ + k_-)t\right] \end{aligned} \tag{26}$$

from which it is clear that in general the dwell time will have an exponential distribution whose mean is $1/\sum_i k_i$.

The dwell time MC algorithm produces a random sample from this exponential distribution using a random number, r_1, uniformly distributed in the domain $[0, 1]$ and transforming to a dwell time using

$$\mathcal{T}(r_1) = -ln(r_1)/(k_+ + k_-). \tag{27}$$

Once the dwell time, $\mathcal{T}$, is known a second random number, r_2, uniformly distributed in the domain $[0, 1]$ is used to determine the type of transition which occurs at $\mathcal{T}$. The domain $[0, 1]$ is split into regions of size $p_i = k_i / \sum_i k_i$ and a logical test to see which of these regions r_2 falls within determines the type of transition.

Again the position of the motor is altered accordingly and the process is repeated.

3 Results and Discussion

3.1 ATPase Synthesis Rate

In order to validate the model it was tested against experimental data. This was done using data for the ATPase synthesis rate under varying ΔG_0 taken from Junesch and Graber [1991]. This data was chosen as the change in ΔG_0 was acheived by varying the internal pH while keeping the external pH constant. This assay is important as it is expected that k_{0+} would not be constant as defined in our model under varying external pH. The internal pH and $\Delta\psi$ dependence is however contained in the $\exp[\Delta G/k_B T]$ term in the model. The parameters used in the MC simulation to produce the fit shown in figure 9 were $u_0 = 2\pi/14$ rad, $u_1 = 2\pi/3$ rad, $k_{0+} = 1820\ s^{-1}$, $k_{1+} = 1050\ s^{-1}$, $\Delta G_1 = -48$ kJ M^{-1} and $\lambda = 30$ pN nm rad^{-1}.

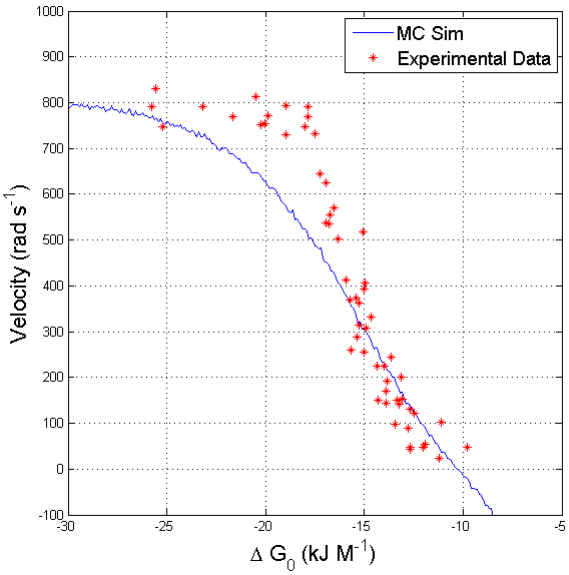

Figure 9: Comparison of experimental data and the MC sim for velocity against ΔG_0

Agreement to the experimental data is seen at two crucial points. First, the thermodynamic equilibrium where the velocity of the ATPase is zero agrees well with the experimental data and also agrees with the theoretical value of $\Delta G_0^{equi} = \Delta G_1 u_0 / u_1 = -10.3$. Second, the maximum ATPase velocity achieved by both the experiment and the MC simulation is ≈ 800 rad s^{-1} which is in agreement with the maximum rate calculated from $u_0 k_{0+}$ as expected (section 1.6). The MC simulation does not acheive this maximum rate as quickly as the actual ATPase however resulting in a less prominent 'elbow'. This is believed to be symptomatic of the simplification

of a complex multi step process into single step with constant rate and the approximation to a B-type motor.

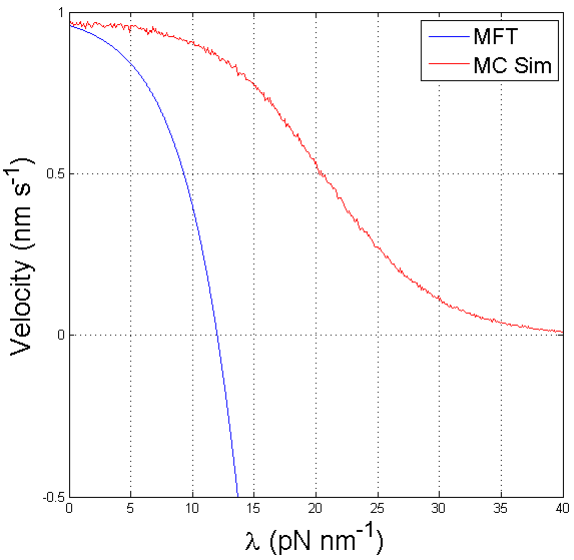

Figure 10: Comparison of the MFT and the MC sim for velocity against λ

The set of arbitrary values given in section 1.6 were used to plot the velocity of the ATPase against λ for comparison to the MFT. The MC simulation shows good agreement as $\lambda \to 0$, as expected, but there is rapid deviation in the simulated velocity. However, with the thermodynamic constraint preventing negative velocities applied to the MFT the two methods agree qualitatively and as λ increases the velocity in both cases decays to zero.

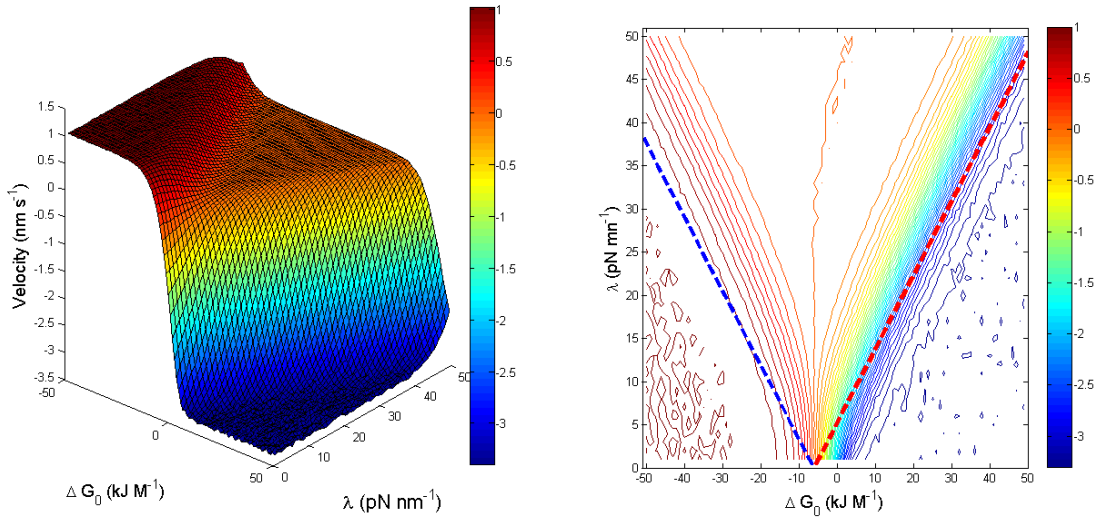

(a) Surface plot

(b) Contour plot showing MFT Stalling points

Figure 11: MC Simulation of ATPase velocity against λ and ΔG_0

Both the change in velocity with respect to ΔG_0 and the change in velocity with respect to λ presented can

be thought of as cross sections of a two dimensional surface plot of velocity against ΔG_0 and λ (figure 11a). This is more clearly represented as a contour plot in figure 11b. The thermodynamic equilibrium in this case is given by $\Delta G_0^{equi} = \Delta G_1 u_0/u_1 = -6.0$. These plots resemble a phase diagram with three distinct phases which will be referred to as the forward phase where the velocity is positive and ATP synthesis occurs, the backward phase, where the velocity is negative and protons are pumped across the membrane and the locked phase where the velocity is close to zero. It is interesting to note that there are no thermodynamic constrains preventing forward velocities in the region $\Delta G_0 < \Delta G_0^{equi}$ and equally there are no thermodynamic constraints on backward velocities for $\Delta G_0 > \Delta G_0^{equi}$. In fact for $\Delta G_0 > 0$ protons would naturally diffuse across the membrane without coupling to an ATP hydrolysis reaction. Even so the presence of a locked phase in this region is evidence of the significant role the axle plays in the functioning of the ATPase.

The two functions superimposed on the contour plot in figure 11b appear to indicate the onset of the phase transition to the locked phase. These are calculated from the zero velocity conditions of ATPase when treated with the MFT method. This condition is is met when the operating point (figure 7a) is at zero velocity which is also the equilibrium point of both motors. Consider the force λx at the equilibrium point of the B-type ratchet F_0,

$$\lambda x = -(\Delta G_0 + \frac{1}{2}\lambda u_0^2)/u_0. \tag{28}$$

Setting this equal to λx for the equilibrium point of F_1 we can derive

$$\Delta G_0^{stall} = \frac{u_0}{u_1}\Delta G_1 - \frac{1}{2}\lambda(u_1 - u_0)u_0, \tag{29}$$

to be the 'stalling point' for the forward phase, as calculated by the MFT, and is shown in blue on figure 11b. A similar treatment for the backward phase produced the stalling point shown in red.

3.2 Time Series

One of the benefits of a MC simulation of ATPase is the ability to view the sequence of transitions in time. This is not yet possible in experiments on ATPase but has proved an invaluable tool in the understanding of other coupled pairs of motors. A particular example of this is dynein which has been shown to exhibit both stochastic and coordinated stepping in this way [Reck-Peterson et al., 2012] [Yildiz et al., 2012]. Figure 12a is an example of such a time series for the biological parameters $u_0 = 2\pi/10$ rad, $u_1 = 2\pi/3$ rad, $k_{0+} = 1300\ s^{-1}$, $k_{1+} = 1050\ s^{-1}$, $\Delta G_0 = -20$ kJ M^{-1}, $\Delta G_1 = -48$ kJ M^{-1} and $\lambda = 30$ pN nm rad^{-1}. Three key observations can be drawn from figure 12.

- The overall behavior exhibited in Figure 12a is of a 'stick slip' nature which it is proposed could be modeled by considering the F_1 to be a fixed support to which the F_0 is tethered. Once the F_0 has made enough forward steps to provide the necessary force in the axle for a single ATP synthesis the F_1 support moves one step and the process is repeated (Section 3.3).

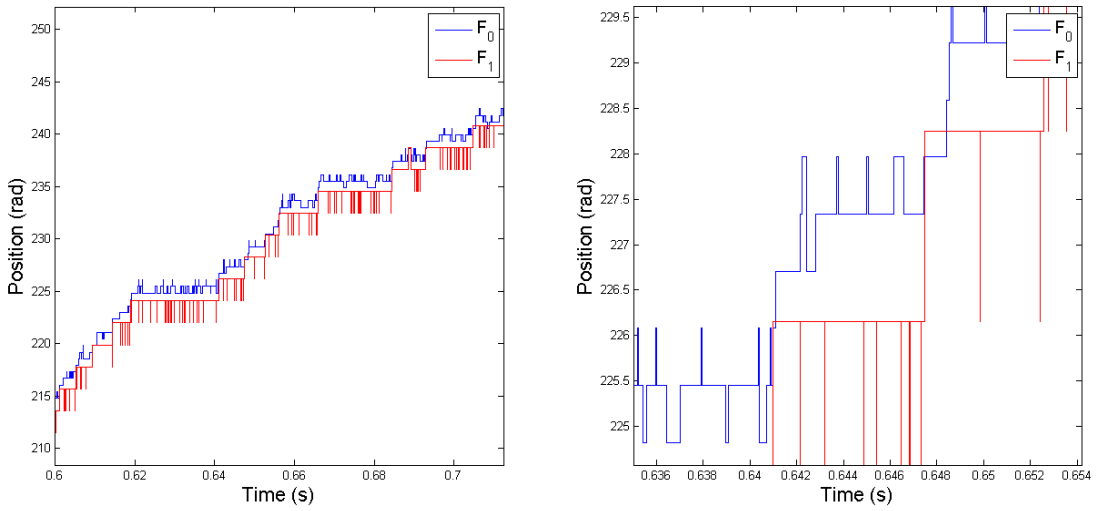

(a) Time series of F_0 and F_1 transitions

(b) Detailed view

Figure 12: Time series plots

- The detailed behavior shows occasional overlapping of the motors and for very brief times the F_1 leads the F_0. This is considered remarkably like the heavily correlated behavior of 'Hand over Hand' type molecular motors such as dynein. A study of the correlation of the motors will hope to confirm this (Section 3.4).
- Both motors exhibit very high frequency 'flip flop' type behavior producing tension fluctuations in the axle. Understanding these tension fluctuations may inform the development of the MFT (Section 3.5).

3.3 Tethered Motor Rate

Consider a single B-type motor tethered to a ridged support by a spring. This motor will perform a restrained random walk but with an analytical solution for the probability of site occupation

$$p(n) = \exp\left[E_n/k_BT\right]/\mathcal{Z}, \tag{30}$$

where $\mathcal{Z}$ is the partition function

$$\mathcal{Z} = \sum_{n=-\infty}^{\infty} \exp\left[E_n/k_BT\right]. \tag{31}$$

The energies for this system are given by

$$E_n = -(\Delta G_0 n + \frac{1}{2}\lambda((nu_0)^2 + x^2)) \tag{32}$$

which yields a Gaussian probability distribution with a mean $n = -\Delta G_0/(\lambda u_0^2)$. The time it takes for this motor to perform enough forward steps to produce the force required to synthesis a single ATP molecule is a compound dwell time and can either be calculated analytically or using a MC simulation. For a u_0:u_1 ratio of 3:1 the tether (F_1) would move every time the motor reached the third site from the origin. A MC simulation

was written to find this 'three step dwell time' and it's reciprocal averaged over many trials was used as the rate of the tethered motor model. If it were possible to simplify the model of ATPase by identifying this as a rate limiting process, which can be solved analytically, this would be a great success.

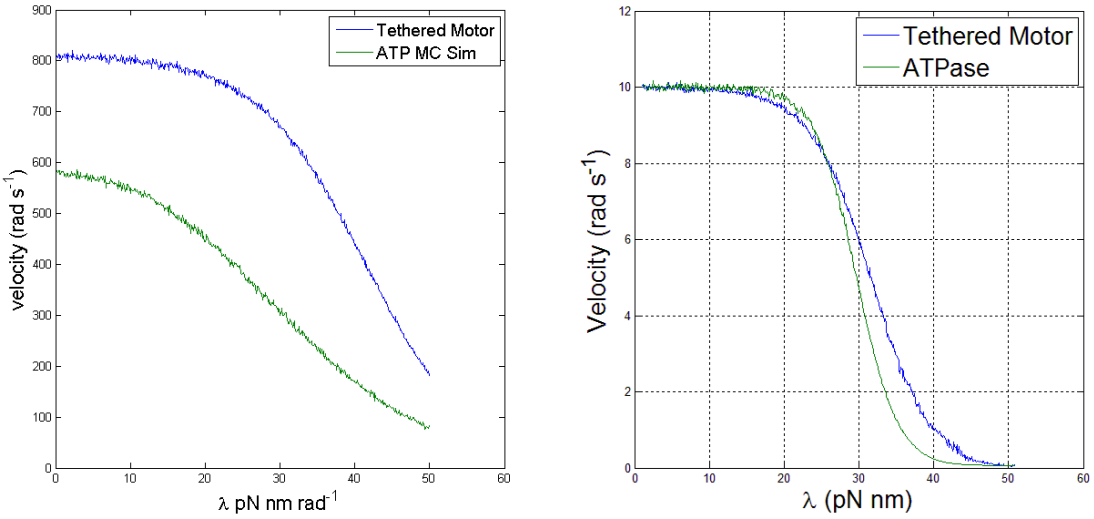

(a) Biological parameters

(b) Arbitrary parameters

Figure 13: Tethered Rate

Early indications using arbitrary parameters proved convincing (figure 13b) however it was found that this was a special case and the conditions which must be met for this method to be considered a rate limiting process are extensive. As observed in section 3.1 the onset of the phase transition appears to be related to equation 29 which is proportional to ΔG_1 which is currently not taken account of in the tethered motor. There is no dependence on u_1 in this method either and though this has not been considered to date the ratio u_0:u_1 has been considered and found to be critical to this method. The tethered motor model currently only applies to integer ratios and for non-integer ratios it either over or under estimates the rate. Consider for example the 10:3 ratio commonly used in this study and applicable to human ATPase. Every third F_1 step will require four F_0 steps to maintain the free energy balance and the mean torque in the axle. A four step dwell time is longer than a three step dwell time and so the tethered rate will be an over estimate. This is the most typical result of the tethered motor model and is shown in figure 13a for the biological parameters.

Algorithms for counting 'transition types' have been included in ATPase Application which may be of use in the future to characterise the sequences of transitions that lead to an ATP synthesis. Data for the types of transitions and there frequency may be useful in future work improving the tethered motor model by mixing rates for different transition sequences. This would have to include not only the occasions when more tethered motor transitions are required but also the number of transitions which involve the overlapping of the F_0 F_1 motors which will have the effect of increasing the rate of the ATP synthesis.

The investigation of this method also highlights a limitation in the ATPase model as when integer ratios u_0:u_1 are used artefacts including an ability to synthesis ATP even at the largest values of λ tested. This is believed to be due to false degeneracies in the energies of adjacent states which only appear at integer ratios. It is not proposed that this has any physical significance to ATPase.

3.4 Auto-Correlation

We can see from the time series data (section 3.2) that the motors 'flip flop' between states while waiting between forward transitions. As discussed, when forward transitions do occur, F_1 often overlaps F_0 meaning the F_1 briefly leading the F_0 in a 'Hand over Hand' type motion. This alternated stepping is believed to contribute to the ability of the ATPase to synthesis at larger values of λ than the MFT suggests and should be evident by a strong correlation between the motors.

The correlation for a time lag τ is given by

$$R_c(\tau) = \langle x_0(t).x_1(t+\tau)\rangle, \tag{33}$$

which is normalised by the variance to give the correlation coefficient. The auto correlation is the correlation of a function with itself and is calculated using $x_0(t) = x_1(t)$. As the time between transitions is random we find that little information is retained when the correlation is calculated for a time series. It is more convenient to consider the behavior in what we term 'transition space' where each transition is a single unit in transition space. In this case the lag, τ, is no longer measured in time but in transitions. This method retains all the information about the sequence of events which occur without being smeared out by the different dwell times between the events.

For the F_0 auto-correlation, the F_1 auto-correlation and the F_0F_1 cross-correlation we have been unsuccessful in isolating the fluctuations seen in the time series data from the correlation function of the drift of the system as a whole. A number of methods have been attempted including subtracting the drift velocity from each of the points in the sequence prior to correlation and subtracting the correlation function of the drift velocity from the correlation function after its calculation. Some progress has been made and correlation functions typical of the fluctuations seen in the time series have been observed superimposed on other residual correlation functions but no value has been put on these observations as of yet. Instead we are able to look at the auto-correlation of the angular deflection of the axle. This is still not ideal as it is difficult to separate out the combined information from fluctuations of the F_0 and the F_1 motors contained in this data. An example of an attempt to do so however is shown in figure 14. The auto-correlation coefficient of x, the angular deflection, in transition space, for the biological parameters previously discussed, but with a vastly reduced forward F_1 rate ($\sim 10s^{-1}$) was plotted for three different values of λ. The rate of F_1 was reduced so that the motor would not fluctuate about

its equilibrium position while waiting between transitions. The forward rate behavior of the ATPase model was largely unaffected by this alteration. The results in figure 14 show a representative sample of the behavior even without the correction to the F_1 rate. In general for small values of λ the correlation function decayed rapidly with what appears to be an exponential as expected for a system governed by Brownian motion [Reif, 1965]. For increasing λ however we see an oscillating function with a frequency of 0.5 Transitions^{-1} which increases in magnitude with λ. At very long lags ($\sim 10^4$, figure 14d) we see that even for large λ this oscillation also decays exponentially to an uncorrelated state.

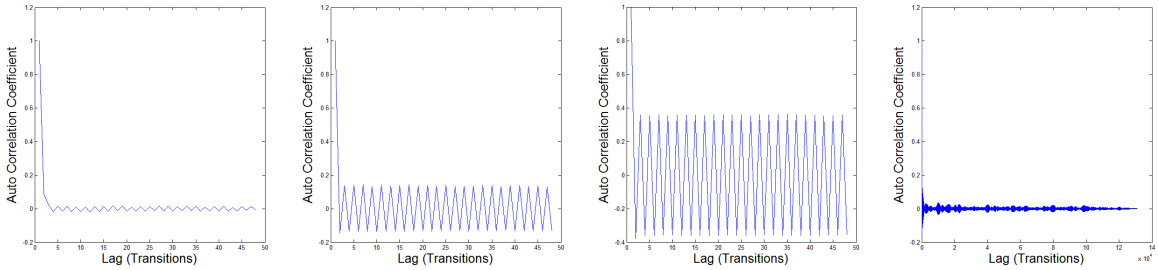

(a) $\lambda = 5$ pN nm rad^{-1} (b) $\lambda = 30$ pN nm rad^{-1} (c) $\lambda = 60$ pN nm rad^{-1} (d) $\lambda = 60$ pN nm rad^{-1} up to transition lags of 10^{14}

Figure 14: Auto-Correlation coefficients for the angular deflection of the axle

3.5 Frequency Analysis

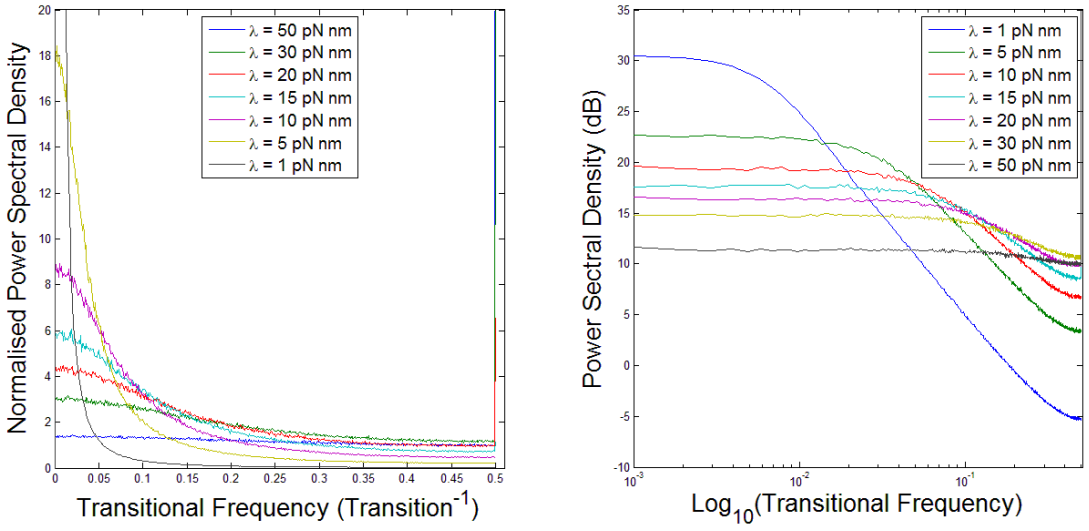

(a) (b)

Figure 15: Power Spectral Densities of Transition fluctuations

The oscillating behavior of the auto-correlation function and the fluctuation in the time series data suggest that frequency analysis of the transitions may yield important information about the function of ATPase. As with the correlation functions the frequency analysis was carried out in the 'transition space'. Figure 15a shows the power spectral density of the transitions at a range of λ. This was done using Danielson-Lanczos method [Press

et al., 2007] converted for C# to perform fast Fourier transforms on transition sequences. For large λ (> 20 pN nm rad^{-1}) a peak in the spectrum can be seen at 0.5 transition^{-1} as anticipated from the correlation functions. Further detail however is provided by the frequency spectra for the smaller values of λ. The same data is shown in figure 15b on a dB with reference value 0.1 to Log_{10} plot. From this we can see that at small values of λ the power spectrum follows a -20dB per Decade law which confirms the previous statement that the motors were subject to Brownian type motion in this regime. As λ is increased the 0.5 transition^{-1} peak is observed and the background frequency dependence tends towards low intensity white noise. This is remarkably reminiscent of the work by Reck-Peterson et al. [2012] which suggests dynein can behave both stochastically and coordinately in different regimes.

As a point of interest it has been observed that power spectral density of the tethered motor is identical to that of the ATPase axle (figure 16a). Also, the correlation and frequency analyses were cross checked for completness through the use of the Wiener-Khintchine relation

$$PSD(\nu) = \int_{-\infty}^{+\infty} R_c(\tau) \exp\left[-2i\pi\nu\tau\right] d\tau \tag{34}$$

which allows the power spectral density function ($PSD(\nu)$) to be calculated by taking the Fourier transform of the correlation function.

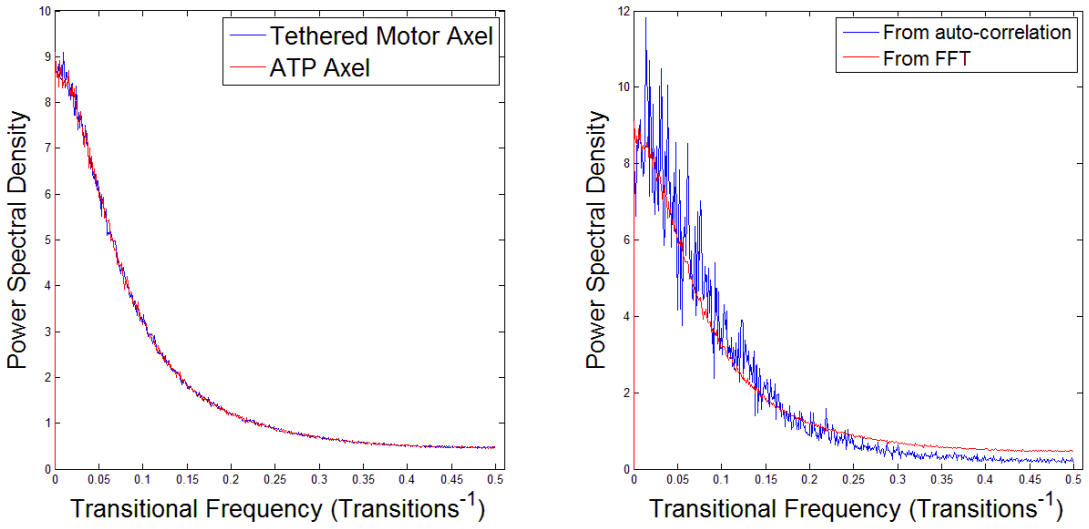

(a) Power Spectrum of the Tethered Motor

(b) Implementation of Wiener-Khintchine

Figure 16: Other interesting frequency analysis

4 Conclusions

The aim of this project was to produce a model for the rate of the F_0F_1ATP Synthase and to explore the conditions required for F_0 and F_1 to work together effectively to synthesis ATP. Using a 'tug of war' between

two chemically driven ratchets with constant forward rates as a model and efficient Monte-Carlo algorithms to simulate this model, experimental data for the rate of ATP synthesis has been reproduced at and far away from the thermodynamic equilibrium.

Three phases of operation of the ATPase model have been identified, the forward ATP synthesising phase, the backward proton pumping phase and the locked zero velocity phase. Given the lack of thermodynamic constraints in this locked phase it is determined that the torsional rigidity of the γ-subunit and the energy required to rotate this subunit by a given discrete step size is responsible for the locking of the motor. Conditions for the onset of this locked phase (section 3.1) have been proposed using the mean field theory outlined in section 1.6.

A possible rate limiting process which could be solved analytically to determine the rate of ATP synthesis has been proposed based on the compound-step dwell times a single B-type motor tethered to a fixed support. This model has not yet been considered rigorously enough to fully formulate as a theoretical model for ATPase.

Both the auto-correlation function and the power spectral density of the fluctuations in the angle of the γ-subunit suggest that like the coupled dynein motors the ATPase operates in two different regimes. The first, at small values of λ is a stochastic, uncorrelated regime where the fluctuations of the motors and the γ-subunit obey Brownian statistics. The second is a correlated regime where alternated stepping and a strong peak in the power spectral density at 0.5 transition^{-1} allows the ATPase to continue working effectively beyond the predictions made using the mean torque of γ.

5 Proposal For Continuation of Study

The scope for future work on improving this model is significant. To date no consideration has been given to evidence such as that provided by Kinosita et al. [1998b] that the rotation of the F_1 motor is in fact composed of substeps of 30^o and 90^o. It is highly likely that the inclusion of F_1 substeps will promote the rate of synthesis with respect to λ (equation 29 for the onset of the phase transition). This would make the larger values of λ quoted in more recent experimental literature [Junge et al., 2008] more suitable for use in this model. Experimental work to determine the rate constants or force-velocity relations of the sub steps would be needed for future refinement of the model.

Continued transitional analysis, as discussed in section 3.3, should be carried out in order to inform the mixing of tethered motor rates required to make this model more rigorous.

Finaly, Previous work by Thomas and Thornhill [1995] shows it is possible to introduce Langevin noise terms [Reif, 1965] into steady state rate equations of muscle cross bridges to model tension fluctuations. The tension fluctuations in this model are significantly larger than in the muscle cross bridge model so the strength of the

noise terms will be much larger but this may improve the estimates of the MFT.

References

C. H. Berg. Random walks in biology. *Princeton University Press*, 1993.

R. M. Berry. Theories of rotary motors. *Phil. Trans. R. Soc. Lond. B*, 355, 2000.

R. M. Berry, W. S. Ryu, and H. C. Berg. Torque-generating units of the fagellar motor of Escherichia coli have a high duty ratio. *Nature*, 403, January 2000.

A. V. Bobylev and C. Cercignani. Moment equations for a granular material in a thermal bath. *Journal of Statistical Physics*, 106, February 2002.

P. D. Boyer. The ATP Synthase - a splendid molecular machine. *Annu. Rev. Biochem.*, 1997a.

P. D. Boyer. Energy, Life, and ATP. Nobel Lecture, 1997b.

Columbia University. Biological sciences at columbia university, index. `http://www.columbia.edu/cu/biology/courses/c2005/images/`, Accessed December 2011.

G. Deckers-Hebestreit and K. Altendorf. The F_0 complex of the proton-translocating F-type ATPase of escherichia coli. *J. exp. Biol*, 172, 1992.

J. Howard, A. J. Hudspeth, and R. D. Vale. Movement of microtubules by single kinesin molecules. *Nature*, 342, 1989.

H. E. Huxley. The mechanism of muscle contraction. *Science*, 164, June 1969.

U. Junesch and P. Graber. The rate of ATP-synthesis as a function of δpH and $\delta\psi$ catalyzed by the active, reduced H^+-ATPase from chloroplasts. *FEBS*, 294, December 1991.

W. Junge, DA Cherepanov, and A Mulkidjanian. Transient accumulation of elastic energy in proton translocating ATP synthase. *FEBS Lett*, 499, 1999.

W. Junge, H. Sielaff, H Rennekamp, A. Wachter, H. Xie, F. Hilbers, K. Feldbauer, S. D. Dunn, and S. Engelbrecht. Domain compliance and elastic power transmission in rotary F_0F_1-ATPase. *PNAS*, 105, November 2008.

G. Karp. *Cell and Molecular Biology.* Wiley, 2008.

Jr. K. Kinosita, H. Noji, R. Yasuda, and M. Yoshida. Direct observation of the rotation of ϵ subunit in F_1-ATPase. *Nature*, 386, January 1997.

Jr. K. Kinosita, H. Noji, R. Yasuda, Y. Kato-Yamada, and M. Yoshida. Direct observation of the rotation of ϵ subunit in F_1-ATPase. *Journal of Biological Chemistry*, 278, July 1998a.

Jr. K. Kinosita, H. Noji, R. Yasuda, and M. Yoshida. F_1-ATPase is a highly efficient molecular motor that rotates with discrete 120^o steps. *Cell*, 93, June 1998b.

Jr. K. Kinosita, N. Mitome, H. Noji, E. Muneyuki, R. Yasuda, T. Masaike, and M. Yoshida. Rotation of F_1-atpase and the hinge residues of the β subunit. *The Journal of Experimental Biology*, 203, 2000.

Jr. K. Kinosita, T. Suzuki, H Ueno, and M. Yoshida. ATP-driven stepwise rotation of F_0F_1-ATP synthase. *PNAS*, 102, Feburary 2005.

I. Lerner. Phase transitions. Lecture Course, 2011.

H. Lill, S. Engelbrecht, G. Schonknecht, and W. Junge. The proton channel, CF_0, in thylakoid membranes. *Eur. J. Biochem*, 160, June 1989.

F. Lipmann. Metabolic generation and utilization of phosphate bond energy. *Adv. Enzymol.*, 1, 1941.

M. Matsumoto and T Nishimura. Mersenne twister: a 623-dimensionally equidistributed uniform pseudo-random number generator. *TOMACS*, 8, January 1998.

N. Metropolis and S. Ulam. The monte carlo method. *Journal of the American Statistical Association*, 44, September 1949.

Jayati Mookerjee-Basu, Pierre Vantourout, Laurent O. Martinez, Bertrand Perret, Xavier Collet, Christian Perigaud, Suzanne Peyrottes, and Eric Champagne. F_1 adenosine triphosphatase displays properties characteristic of an antigen presentation molecule for vγ9vδ2 T cells. *The Journal of Immunology*, 184, May 2010.

MSDN Website. Introduction to the C# language and the .net framework. `http://msdn.microsoft.com/library/z1zx9t92`, Accessed March 2012.

D. G. Nicholls and S. J. Ferguson. *Bioenergetics 2.* Academic Press, London, San Diego, 1992.

O. Pänke and B. Rumberg. Kinetic modeling of rotary CF_0F_1-ATP synthase: storage of elastic energy during energy transduction. *Biochimica et Biophysica Acta*, 1412, 1999.

W. H. Press, S. A. Teukolsky, W. T. Vetterling, and B. Flannery. *Numerical Recipes in C.* Cambridge University Press, 2007.

S. L. Reck-Peterson, W. Qiu, N. D. Derr, B. S. Goodman, E. Villa, D. Wu, and W. Shih. Dynein achieves processive motion using both stochastic and coordinated stepping. *Nature Structural and Molecular Biology*, January 2012.

F. Reif. *Fundamentals of statistical and thermal physics.* McGraw-Hill, 1965. chap. 15.

M. Rief, R. S. Rock, A. D. Mehtta, M. S. Mooseker, R. E. Cheney, and J. A. Spudich. Myosin-V stepping kinetics: a model for processivity. *Proc. Natl Acad. Sci.*, 2000.

N. Thomas. Lecture 2, chemical reactions. Y3 Biological Nano-Machines Lecture Course, 2011a.

N. Thomas. Lecture 4, ratchets. Y3 Biological Nano-Machines Lecture Course, 2011b.

N. Thomas and R. A. Thornhill. Tension fluctuations due to muscle cross-bridges. *Proceedings: Biological Sciences*, 259, march 1995.

N. Thomas and R. A. Thornhill. The physics of biological nanomotors. *J. Phys. D: Appl. Phys.*, 31, 1997.

N. Thomas, Y. Imafuku, and K. Tawada. Molecular motors: thermodynamics and random walk. *Proc. R. Soc. Lond. B*, 268, June 2001.

J. E. Walker. ATP Synthesis by Rotary Catalysis. Nobel Lecture, 1997.

J. E. Walker, D. Stock, and A. G. W. Leslie. Molecular architecture of the rotary motor in atp synthase. *Science*, 286, November 1999.

M. L. Walker, S. A. Burgess, J. R. Sellers, F. Wang, J. A. Hammer, J. Trinick, and P. J. Knight. Two-headed binding of a processive myosin to f-actin. *Nature*, 405, 2000.

A. Yildiz, M. A. DeWitt, A. Y. Chang, and P. A. Combs. Cytoplasmic dynein moves through uncoordinated stepping of the AAA+ ring domains. *Science*, 335, January 2012.

6 Appendices

A Algorithms

A.1 Random Walk

```
double rwkplus = 0.1;
            double rwkminus = 0.4;
            double rwdt = 0.001/(rwkplus+rwkminus);//time step
            double rwdpminus = rwkminus*rwdt;//prob of forwards step
            double rwdpplus = rwkplus*rwdt;//prob of backwards step
            double rwdpnomove = 1-(rwdpminus + rwdpplus);// prob of no move
            double[] rwtime = new double[MaxTransitionsNumber];//time
            double[] rwpos = new double[MaxTransitionsNumber];//position
            rwtime[0] = 0;
            rwpos[0] = 0;
            Random seeding = new Random();
            int seed = seeding.Next();
            MersenneTwister rand = new MersenneTwister(seed);
```

```
            for (int i = 1; i < MaxTransitionsNumber; i++)
            {
                double r = rand.NextDouble();//random number [1,0]
                if (r < rwdpnomove)
                { rwtime[i] = rwtime[i - 1] + rwdt; rwpos[i] = rwpos[i - 1]; }//no move
                //else if backwards step
                else if (r > rwdpnomove && r < (rwdpnomove + rwdpminus))
                {
                    rwpos[i] = rwpos[i - 1] - 1;
                    rwtime[i] = rwtime[i - 1] + rwdt;
                }
                //else there is a forwards step
                else
                {
                    rwpos[i] = rwpos[i - 1] + 1;
                    rwtime[i] = rwtime[i - 1] + rwdt;
                }
            }
            //plot results
            chart15.Series["Series1"].Points.DataBindXY(rwtime, rwpos);
```

A.2 Dwell Time

```
//initialise the random number generator
            Random seeding = new Random();
            int seed = seeding.Next();
            MersenneTwister rand = new MersenneTwister(seed);
            //initialise variables
            T[0] = 0;
            int n0 = Convert.ToInt32(-dG0 / (lambda * u0 * u0));
            n[0] = n0;
            m[0] = 0;
            x0[0] = n[0] * u0;
            x1[0] = m[0] * u1;
            x[0] = x0[0] - x1[0];
            AVESpringLength = 0;
            //calculate the constant K_+i
```

```
double k0 = kplus0 * Math.Exp((dG0 - 0.5 * lambda * u0 * u0) / kT);
double k1 = kplus1 * Math.Exp((dG1 - 0.5 * lambda * u1 * u1) / kT);
//begin the MC routine
for (int j = 1; j < MaxTransitionsNumber; j++)
{
    //rate constants
    double kminus0 = k0 * Math.Exp((lambda * u0 * x[j - 1]) / kT);
    double kminus1 = k1 * Math.Exp((lambda * u1 * x[j - 1]) / kT);
    double r1 = rand.NextDouble();//random number [0,1]
    double r2 = rand.NextDouble();//random number [0,1]
    double dwelltime = -Math.Log(r1) / (kplus0 + kminus0 + kplus1 + kminus1);
    double pplus0 = kplus0 / (kplus0 + kminus0 + kplus1 + kminus1);
    double pminus0 = kminus0 / (kplus0 + kminus0 + kplus1 + kminus1);
    double pplus1 = kplus1 / (kplus0 + kminus0 + kplus1 + kminus1);
    //logical check on the random number in the domain [0,1]
    if (r2<pplus0)
    {
        n[j] = n[j - 1] + 1;
        m[j] = m[j - 1];
    }
    else if(pplus0 < r2 && r2 < (pminus0 + pplus0))
    {
        n[j] = n[j - 1] - 1;
        m[j] = m[j - 1];
    }
    else if ((pplus0 + pminus0) < r2 && r2 < (pplus1 + pplus0 + pminus0))
    {
        m[j] = m[j - 1] - 1;
        n[j] = n[j - 1];
    }
    else
    {
        m[j] = m[j - 1] + 1;
        n[j] = n[j - 1];
    }
    T[j] = T[j - 1] + dwelltime;
```

```
        x0[j] = u0 * n[j];
        x1[j] = u1 * m[j];
        x[j] = x0[j] - x1[j];
        AVESpringLength = AVESpringLength + x[j] * (T[j] - T[j - 1]);
        progressBar1.Value = j * 100 / MaxTransitionsNumber;
    }
    //agregate results
    v0 = x0[MaxTransitionsNumber - 1] / T[MaxTransitionsNumber - 1];
    N = n[MaxTransitionsNumber - 1];
    ATPyeild = N / T[MaxTransitionsNumber - 1];
    AVESpringLength = AVESpringLength / T[MaxTransitionsNumber - 1];
```